Model Predictive Control-Based Three-Port Common Ground Photovoltaic-Battery Grid-Connected Inverter

Mokhtar Aly, Eltaib Abdeen D. Ibrahim, Samir Kouro, Emad Ahmed, Thierry Meynard, Jose Rodriguez

Model Predictive Control-Based Three-Port Common Ground Photovoltaic-Battery Grid-Connected Inverter

Mokhtar Aly[1], Eltaib Abdeen D. Ibrahim[2], Samir Kouro[3], Emad M. Ahmed[4,5]
Thierry A. Meynard[6], Jose Rodriguez´ [7]

[1]*Facultad de Ingenier´ıa y Tecnolog´ıa, Universidad San Sebastian´* , Bellavista 7, Santiago, Chile
[2]*Electrical Engineering Department, High Institute for engineering and technology in Sohag*, Sohag, Egypt
[3] *Electronics Engineering Department, Universidad Tecnica Federico Santa Maria*, Valparaiso 2390123, Chile
[4]*Electrical Engineering Department, Aswan University*, Aswan 81542, Egypt
[5] *Department of Electrical Engineering, Jouf University, College of Engineering*, Sakaka 2014, Saudi Arabia
[6] *Institut National Polytechnique de Toulouse, University of Toulouse*, Toulouse, France
[7] *Universidad Andres Bello*, Santiago, Chile
mokhtar.aly@aswu.edu.eg, e.abdeen@ieee.org, samir.kouro@ieee.org, emad@eng.aswu.edu.eg
thierry.meynard@laplace.univ-tlse.fr, jose.rodriguez@unab.cl

Abstract—Battery energy storage systems (BESSs) have become integral parts in photovoltaic (PV) energy systems due to their fluctuated nature. The most common solutions in the literature for hybrid PV-battery systems are based on twostage power converter solutions with separate power converters. However, these solutions increase the cost of the system and the number of required devices. Additionally, leakage currents represent critical issue for safe and reliable operation of PV systems. This paper presents a three-port configuration for hybrid PV-battery grid-connected systems. The proposed configuration includes a common ground connection between the PV side and grid side, which results in the elimination of leakage current components. Moreover, a finite control set model predictive control (FCS-MPC) is presented in this paper for controlling the proposed three-port configuration. The proposed controller achieves the control of multiple objectives simultaneously in addition to having fast dynamic response. Simulation results of the proposed configuration and control method are provided in this paper. The results show the effectiveness of the proposed configuration for hybrid PV-battery systems.

Index Terms—battery energy storage systems (BESSs), common grounded , model predictive control (MPC), photovoltaic (PV), three-port inverter.

I. Introduction

Recently, photovoltaic (PV) systems have found wide concerns all over the world [1], [2]. However, the fluctuated nature of PV systems represents a critical issue for PV installations. The output power of PV systems is dependent on the solar irradiance and ambient temperature. Therefore, battery energy storage systems (BESSs) have become essential parts for maximizing the power extraction and ensuring reliable power supply for the connected loads. From another side, the integration schemes of PV, BESS, and grid sides represent important parts for cost-effective, reliable, and stable operation of the hybrid system [3].

Additionally, the resulting leakage currents represent important factor in the selection process of grid connected PV inverter topologies [4]. common ground (CG) based topologies have been proposed in literature for eliminating leakage currents [5]. In CG inverters, the neutral terminal from grid side is directly connected to the negative terminal from PV side. Hence, the resulting common mode voltages equal to zero and leakage currents are eliminated in accordance [6]. The split source CG topology has been proposed in [7] for achieving high boosting factors, and its enhanced modulation method has been presented in [8]. Several control methods have been presented for CG PV topologies using classical control systems [9]. Whereas, model predictive control (MPC) has proven superior performance for CG PV inverter due to its ability to control multiple objectives simultaneously, while achieving fast dynamic response [10]. The MPC has been also applied for hybrid PV-BESS systems in [11].

Therefore, this paper presents a three-port configuration (TPC) with finite control set (FCS) MPC method for hybrid PV-battery grid connected systems. The proposed configuration is based on using a single power stage with two dc ports (PV and battery) and one ac port (grid side). The proposed configuration represents a low cost, high efficiency, and low component count solution for three-port applications. The FCS-MPC achieves simultaneous control of the various objectives in the system for the three ports. Additionally, reactive power injection to the utility grid is considered in the proposed control method.

The remaining of the paper is organized as follows: Section II presents the proposed three-port configuration and its operating states. The proposed FCS-MPC method is presented in Section III. Section IV shows the obtained simulation results of the proposed configuration and controller. The paper is concluded in Section V.

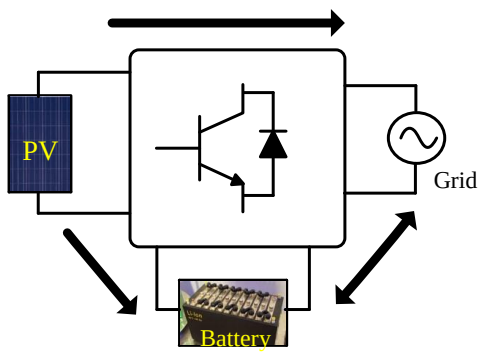

Fig. 1: The schematic diagram of TPC configuration.

II. The Proposed TPC Configuration

A. The Power Circuit

Fig. 1 shows the schematic diagram of the proposed TPC system with hybrid PV-BESS. The PV system is responsible for supplying the power for the battery and the grid based on the outputted power from the PV modules. Whereas, the battery system is charged from the PV or the grid. It is also responsible for supplying the grid side requirements at low output power levels from the PV side. Fig. 2 shows the topology of TPC system with PV source, BESS, and grid connection. It is a modified TPC topology based on the split source CG topology in [7]. The topology includes only five power switches, single inductor, and grid filter. This topology can generate three-level output voltage at the output. The topology has four different switching states as shown in Table.
I.

The current of the inductor L_1 has to be controlled to manage the output power from the PV source. The grid current is controlled based on the electrical grid requirements of active and reactive power. The power converter has to participate in the required functions by the utility grid, such as reactive power sharing. The battery system is controlled to supply the difference of the active power between the demanded grid load and the available PV power. The control system has to perform the different functions simultaneously. This, in turn, makes the design of classical control methods more complex and cascaded control structures are essential. In the proposed system, the ability of MPC methods to achieve multiple functions simultaneously is employed to control the proposed TPC and the power transfer between the different ports.

III. The Proposed MPC Method

A. TPC Modelling

Using the aforementioned topology description, the relationship among the outputted voltage of TPC topology and the switching states can be expressed as follows:

$$v_o(k) = (S_4 - S_1 - S_2 + 1)V_{bat}(k) \tag{1}$$

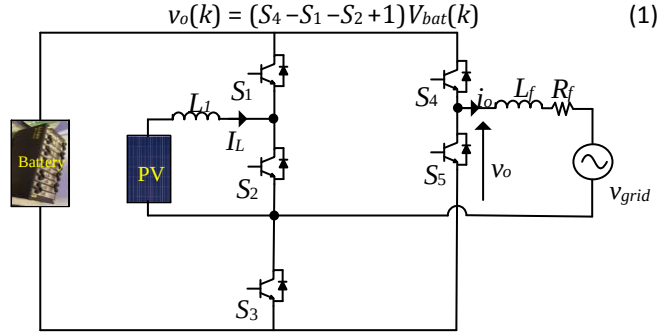

Fig. 2: The connection of power circuit of the proposed TPC configuration.

TABLE I: Switching pulses of the TPC configuration

State No.	v_o	Switches Sign als				
		S_1	S_2	S_3	S_4	S_5
1	V_{bat}	OFF	ON	ON	ON	OFF
2	0	OFF	ON	ON	OFF	ON
3	$-V_{bat}$	ON	ON	OFF	OFF	ON
4	0	ON	OFF	ON	OFF	ON

where, V_{bat} and v_o are the battery, and the outputted voltages of TPC at sampling instant k. Whereas, $S_1 \sim S_5$ are the gating pulse values at any switching instant, wherein their values in (1) equal to one at on-states, and zero at off-states. From another side, the grid-port model is as follows:

$$v_o = v_{grid} + R_f i_o + L_f \frac{di_o}{dt} \tag{2}$$

where, v_{grid} represents the grid voltage. i_o denotes to the injected current from the topology to the grid port. Whereas L_f and R_f are the L-filter inductance and series resistance, respectively. Using the continuous time modelling the the Euler approximation, the grid current can be predicted for the various states as follows:

$$i_o(k+1) = \frac{T_s}{L_f}(v_o(k) - v_{grid}(k)) + (1 - \frac{R_f T_s}{L_f})i_o(k) \tag{3}$$

where, T_s is the sampling period of the MPC method. Whereas, $(k+1)$ and (k) are the $(k+1)^{th}$ and $(k)^{th}$ intervals of sampled grid port current. The grid port current is predicted based on the measured current at sample k and the predicted output voltage using (1).

From another side, the control of the current i_L is predicted for states 1-3 as follows:

$$I_L(k+1) = I_L(k) + \frac{T_s}{L_1}(V_{PV}(k)) \tag{4}$$

where, $I_L(k)$ represents the measured inductor current at sample k, and $V_{PV}(k)$ represents the measured PV voltage. Thence, the inductor current is predicted $I_L(k+1)$ for all states. Whereas, it can predicted for state 4 as follows:

$$I_L(k+1) = I_L(k) + \frac{T_s}{L_1}(V_{PV}(k) - V_{bat}(k)) \quad (5)$$

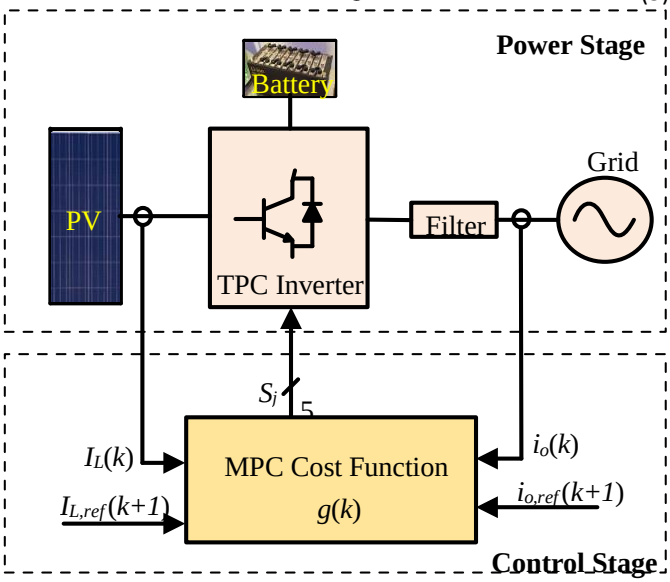

Fig. 3: Block diagram of proposed controller.

The reference current of the PV port $I_{L,ref}$ can be expressed as follows:

$$I_{L,ref}(k+1) = \frac{P_{PV}}{V_{PV}} \quad (6)$$

where, P_{PV} represents the output power of PV at maximum power point tracking. The reference current $i_{o,ref}$ of the grid port is expressed as follows:

$$i_{o,ref}(k+1) = \frac{P_{grid}}{0.5V_{grid(peak)cos(\theta)}} sin(2\pi f_l t + \theta) \quad (7)$$

where, $V_{grid(peak)}$ is the peak value of grid voltage. Whereas, θ represents the power factor angle. It depends on the demanded active power P_{grid} and reactive power Q_{grid} by the grid port and it is represented as fallows:

$$\theta = tan^{-1}\frac{Q_{grid}}{P_{grid}} \quad (8)$$

The injected grid current and the PV current are predicted for the various states of TPC topology. Thence, based on the reference currents, the MPC selects the optimum state for controlling the currents. The gating pulses are generated according to the selected optimum state.

B. The Proposed MPC Controller

The block diagram of the MPC method for TPC topology is shown in Fig. 3. The reference currents are estimated using (6) and (7) for the subsequent sampling instant. The inductor current and the grid current have to be controlled using the MPC method. The two currents are predicted using all the available switching states in the TPC topology. Afterwards, the cost function of the MPC can be expressed as follows:

$$g(k) = \lambda_1(i_{o,ref}(k+1) - i_o(k+1)) + \lambda_2(I_{L,ref}(k+1) - I_L(k+1)) \quad (9)$$

Where λ_1, and λ_2 are the weighting factor values of the grid port current, the PV port current. Afterwards, the switching state that achieves minimized cost function is selected and the corresponding pulses of switches are outputted.

IV. Simulation Results

In this section, the various operating scenarios have been simulated to verify the effectiveness of the proposed topology and controller. The system parameters for the simulated system are summarized in Table II. The simulation results for the proposed topology are designed and simulated using MATLAB/Simulink. A 4KW PV system grid-connected is designed. Different case studies are simulated in order to verify the performance of the proposed system as follows:

(1) PV power changing: In this case study, the inductor reference current is changed by reducing the available power from PV source according to (6) as shown in Fig. 4. It is worth to note that the battery source is controlled to compensate the reduction in the generated power from the PV source. Therefore, the difference power between the demand power and the available power from PV system is supplied. The output voltage and the grid current are still regulated at the same value. Consequently, the inductor current is following the reference according to the change in PV power.

(2) The grid power changing: In this case, the load demand power is reduced by reducing the grid current reference as illustrated in Fig. 5. Therefore, the power output from the battery system is reduced to match the required power from the load side. Its worth to note that the current is in phase with the grid voltage. The output voltage is regulated at 400V without any change. While the inductor current follows the reference and settled at the same value (40A) as long as there is no change in the available PV power. Therefore, the active power is injected to the grid side and controlled properly.

(3) Reactive power changing: in this test, the reactive power is changed from zero to 1.5KW as illustrated in Fig. 6. Therefore, the grid current is not in phase with grid voltage. While the inductor current is regulated and controlled with same reference value.

(4) During this test, The reactive power is controlled at fixed value while, the battery power compensates the difference active power as clear in Fig. 7.

(5) No available PV power and change the reactive power:

The inductor current in this test is zero as long as the available PV power is zero. While the grid current tracked the reference current to control the reactive power as shown in Fig. 8.

V. Conclusions

A three-port power converter configuration is proposed in this paper. The main advantages of the proposed configuration are: it represents a single stage power conversion, the reduced number of components, bidirectional power flow, and reduced cost. In addition, MPC method is proposed in this paper for the proposed configuration. The results show the ability of the proposed controller to control the power flow between the various ports, fast tracking of various currents, and regulation of the grid reactive power requirement.

TABLE II: Parameters of simulation study.

Parameter	Value
PV port voltage V_{PV}	75V
Battery port voltage V_{bat}	400V
Inductance L_1	4.5mH
Line frequency of Grid port f_l	50Hz
Peak-voltage of grid port	311V
Inductance of grid filter L_f	3.5mH
Resistance of grid filter R_f	50mΩ
Sampling frequency of MPC f_s (= $1/T_s$)	50kHz

VI. Acknowledgments

This work was supported by ANID through projects SERC Chile (ANID/FONDAP15110019), AC3E (ANID/Basal/FB0008), FONDECYT 1191532, 11180233, ACT192013 and 1210208.

References

[1] M. Aly and H. A. Ramadan, "Design and implementation of adaptive SVPWM algorithm for multilevel inverters in renewable energy applications," *Solar Energy*, vol. 183, pp. 745–754, May 2019. [Online]. Available: https://doi.org/10.1016/j.solener.2019.03.069

[2] Y. P. Siwakoti and F. Blaabjerg, "Common-ground-type transformerless inverters for single-phase solar photovoltaic systems," *IEEE Transactions on Industrial Electronics*, vol. 65, no. 3, pp. 2100–2111, Mar. 2018.

[3] M. Aly and M. Shoyama, "An efficient neutral point voltage control algorithm with reduced switching losses for three level inverters," in *2014 IEEE International Conference on Power and Energy (PECon)*. IEEE, Dec. 2014. [Online]. Available: https://doi.org/10.1109/pecon.2014.7062466

[4] M. Aly, C. A. Rojas, E. M. Ahmed, and S. Kouro, "Leakage current elimination pwm method for fault-tolerant string h-npc pv inverter," in *IECON 2019 - 45th Annual Conference of the IEEE Industrial Electronics Society*, vol. 1, 2019, pp. 6489–6494.

[5] A. Kadam and A. Shukla, "A multilevel transformerless inverter employing ground connection between pv negative terminal and grid neutral point," *IEEE Transactions on Industrial Electronics*, vol. 64, no. 11, pp. 8897–8907, 2017.

[6] R. Barzegarkhoo, Y. P. Siwakoti, N. Vosoughi, and F. Blaabjerg, "Sixswitch step-up common-grounded five-level inverter with switchedcapacitor cell for transformerless grid-tied PV applications," *IEEE Transactions on Industrial Electronics*, vol. 68, no. 2, pp. 1374–1387, Feb. 2021.

[7] X. Hu, P. Ma, B. Gao, and M. Zhang, "An integrated step-up inverter without transformer and leakage current for grid-connected photovoltaic system," *IEEE Transactions on Power Electronics*, vol. 34, no. 10, pp. 9814–9827, Oct. 2019.

[8] S. S. Lee, Y. P. Siwakoti, C. S. Lim, and K.-B. Lee, "An improved PWM technique to achieve continuous input current in common-ground transformerless boost inverter," *IEEE Transactions on Circuits and Systems II: Express Briefs*, vol. 67, no. 12, pp. 3133–3136, Dec. 2020.

[9] N. Vazquez, J. V´ azquez, J. V´ aquero, C. Hern´ andez, E. V´ azquez, and´ R. Osorio, "Integrating two stages as a common-mode transformerless photovoltaic converter," *IEEE Transactions on Industrial Electronics*, vol. 64, no. 9, pp. 7498–7507, 2017.

[10] J. Zucuni, D. Schuetz, F. Grigoletto, F. Carnielutti, M. Norambuena, J. Rodriguez, and H. Pinheiro, "Modulated model predictive control for three-phase packed-u-cells multilevel converter," in *45th Annual Conference of the IEEE Industrial Electronics Society*, vol. 1, 2019, pp. 1868–1873.

[11] S. Neira, J. Pereda, and F. Rojas, "Three-port full-bridge bidirectional converter for hybrid DC/DC/AC systems," *IEEE Transactions on Power Electronics*, vol. 35, no. 12, pp. 13077–13084, Dec. 2020.

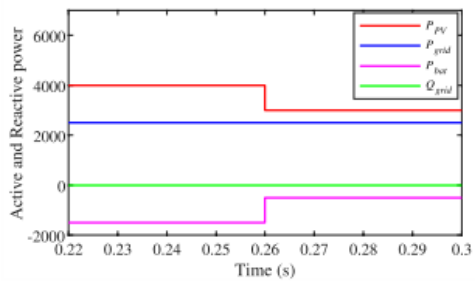

(a) Active and reactive power

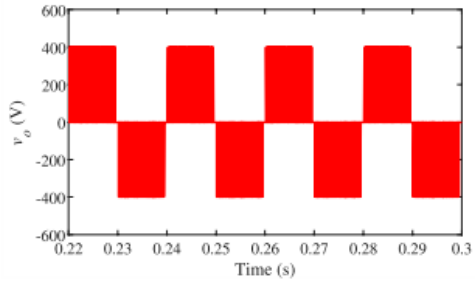

(b) Output voltage

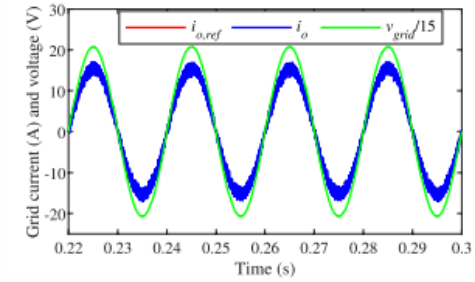

(c) Grid current tracking

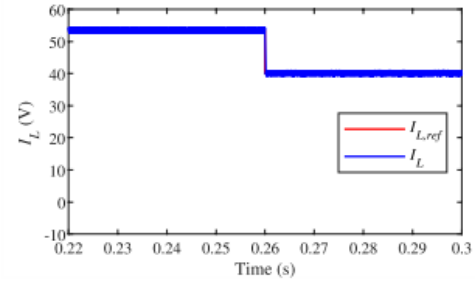

(d) Inductor current tracking

Fig. 4: Simulation results of case 1.

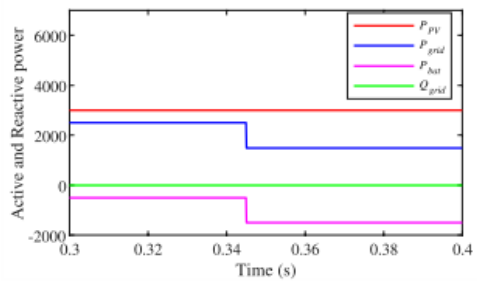

(a) Active and reactive power

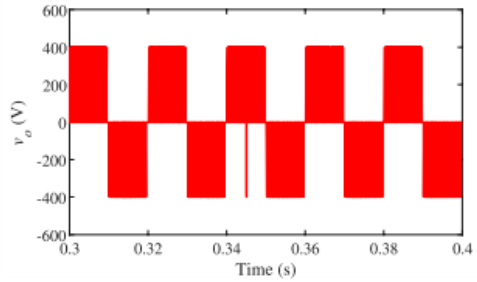

(b) Output voltage

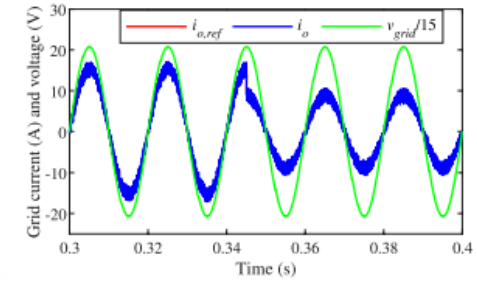

(c) Grid current tracking

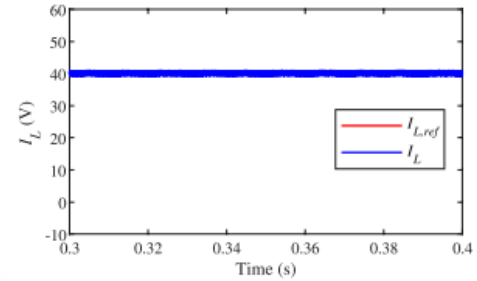

(d) Inductor current tracking

Fig. 5: Simulation results of case 2.

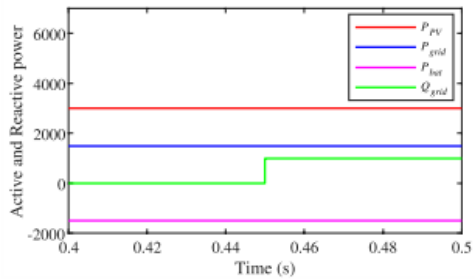

(a) Active and reactive power

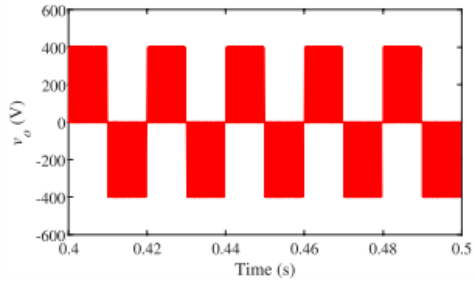

(b) Output voltage

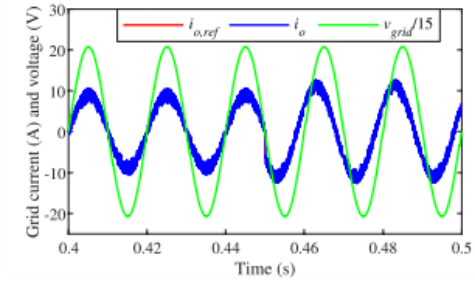

(c) Grid current tracking

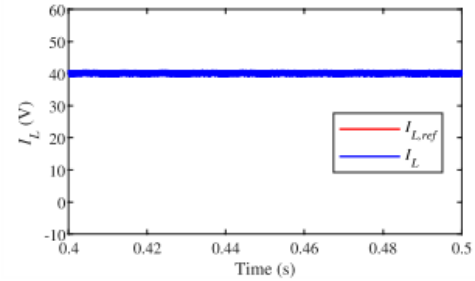

(d) Inductor current tracking

Fig. 6: Simulation results of case 3.

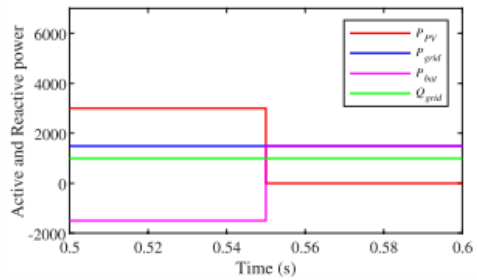

(a) Active and reactive power

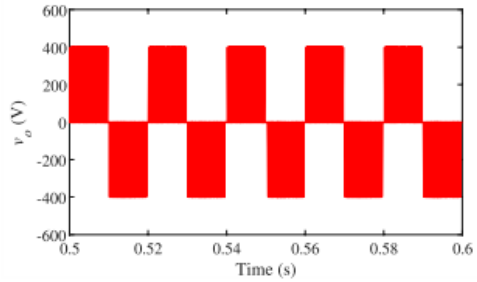

(b) Output voltage

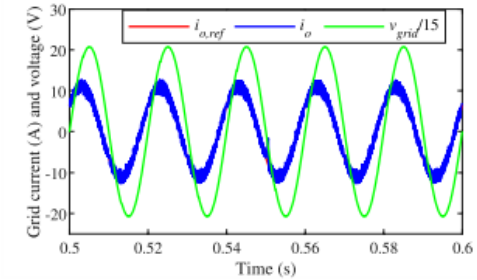

(c) Grid current tracking

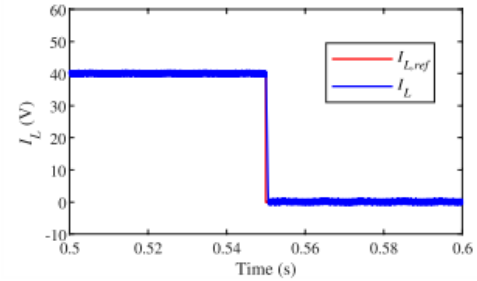

(d) Inductor current tracking

Fig. 7: Simulation results of case 4.

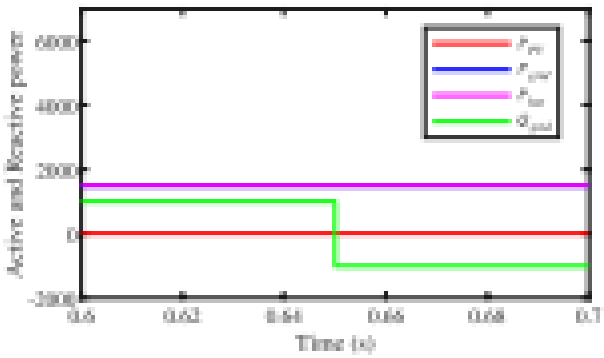

(a) Active and reactive power

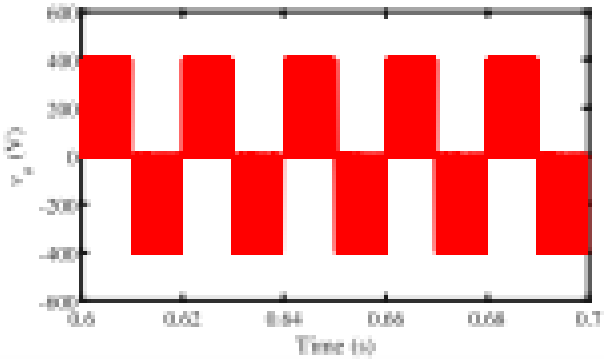

(b) Output voltage

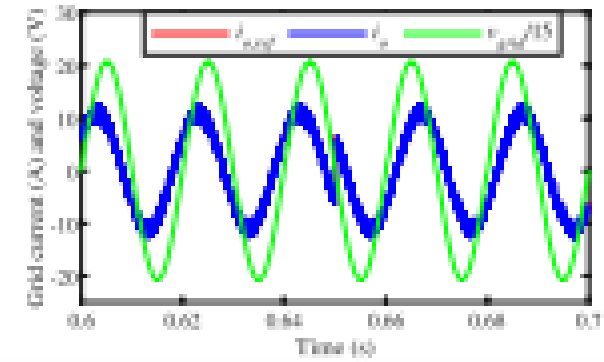

(c) Grid current tracking

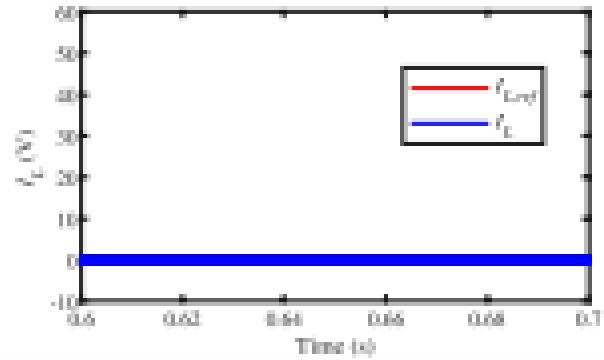

(d) Inductor current tracking

Fig. 8: Simulation results of case 5.